Ecological Monographs, 72(2), 2002, pp. 169–184

DYNAMICS OF MEASLES EPIDEMICS: ESTIMATING SCALING OF TRANSMISSION RATES USING A TIME SERIES SIR MODEL

OTTAR N. BJØRNSTAD,[1] BÄRBEL F. FINKENSTÄDT,[2,3] AND BRYAN T. GRENFELL[3,4]

[1]*Departments of Entomology and Biology, 501 ASI Building, Pennsylvania State University, University Park, Pennsylvania 16802 USA*
[2]*Department of Statistics, University of Warwick, Coventry CV4 7AL UK*
[3]*Department of Zoology, University of Cambridge, Cambridge CB2 3EJ UK*

Abstract. Before the development of mass-vaccination campaigns, measles exhibited persistent fluctuations (endemic dynamics) in large British cities, and recurrent outbreaks (episodic dynamics) in smaller communities. The critical community size separating the two regimes was ~300 000–500 000. We develop a model, the TSIR (Time-series Susceptible–Infected–Recovered) model, that can capture both endemic cycles and episodic outbreaks in measles. The model includes the stochasticity inherent in the disease transmission (giving rise to a negative binomial conditional distribution) and random immigration. It is thus a doubly stochastic model for disease dynamics. It further includes seasonality in the transmission rates. All parameters of the model are estimated on the basis of time series data on reported cases and reconstructed susceptible numbers from a set of cities in England and Wales in the prevaccination era (1944–1966). The 60 cities analyzed span a size range from London (3.3×10^6 inhabitants) to Teignmouth (10 500 inhabitants). The dynamics of all cities fit the model well. Transmission rates scale with community size, as expected from dynamics adhering closely to frequency dependent transmission (''true mass action''). These rates are further found to reveal strong seasonal variation, corresponding to high transmission during school terms and lower transmission during the school holidays. The basic reproductive ratio, R_0, is found to be invariant across the observed range of host community size, and the mean proportion of susceptible individuals also appears to be constant. Through the epidemic cycle, the susceptible population is kept within a 3% interval. The disease is, thus, efficient in ''regulating'' the susceptible population—even in small cities that undergo recurrent epidemics with frequent extinction of the disease agent. Recolonization is highly sensitive to the random immigration process. The initial phase of the epidemic is also stochastic (due to demographic stochasticity and random immigration). However, the epidemic is nearly ''deterministic'' through most of the growth and decline phase.

Key words: epidemic birth–death process; extinction–recolonization; noise and determinism; nonlinear stochastic dynamics; persistence thresholds; population cycles; R_0; spatial coupling; time series analysis; TSIR model.

INTRODUCTION

Over the last two decades, infectious diseases have gained increasing recognition as a key component in the dynamics of populations (reviewed in Anderson and May 1991, Grenfell and Dobson 1995). A number of diseases are endemic in animal populations, that is, they are persistent and almost never go locally extinct. (Note, that we use the word ''endemic'' according to the epidemiological tradition, which is unrelated to the biogeographic usage). The interaction between hosts and their endemic parasites has been modeled intensively. Both host–parasite cycles and reduced host abundance can result from such interactions (Anderson 1978, May and Anderson 1978, Anderson and May 1979). Endemism (local persistence) depends on parasite vital rates, host abundance and host reproduction (e.g., Anderson et al. 1981, Grenfell and Harwood 1997). In essence, such infections can invade if the basic reproductive ratio of infection, R_0, is greater than unity (Anderson and May 1979, 1991, May and Anderson 1979, Schenzle 1984, Heesterbeek and Roberts 1994). Persistence also depends on a sufficiently high replenishment rate of susceptibles to maintain a ''chain of transmission'' (Grenfell and Harwood 1997). A number of diseases, however, appear to be non-endemic. They are characterized by episodic outbreaks followed by local stochastic extinction of the disease, as the chain is broken. Disease persistence in such systems therefore depends on reintroduction of the infection (Cliff et al. 1993, Grenfell and Harwood 1997, Earn et al. 1998). Successful reinvasion into the host population depends again on R_0 being larger than one as the density of susceptibles exceeds some threshold density (Anderson et al. 1981, Grenfell and Dobson 1995). Dense populations are therefore more likely to sustain a disease than sparse populations (Bartlett 1956, 1957,

Manuscript received 5 July 2000; revised 13 April 2001; accepted 30 April 2001; final version received 29 May 2001.
[4] Corresponding author. E-mail: b.t.grenfell@zoo.cam.ac.uk

1960*a*). Endemic persistence is also promoted by a suite of other parasite adaptations such as prolonged infectious periods (Dietz and Schenzle 1985), carrier hosts, etc. (Grenfell and Dobson 1995). The route to local disease extinction is similar to that in predator–prey metapopulations (Grenfell and Harwood 1997)—after introduction, the host supply is depleted to a level where the parasite, or both the host and the parasite, go locally extinct.

The theory of disease dynamics, thus, parallels the frontiers of population ecology at large, by focusing on persistence, extinction, recolonization, and the dynamics of small populations (Earn et al. 1998, Hanski 1998). These processes are key components in a theory for conservation where large-scale density-dependent mechanisms scale down to enter the realm where stochasticity is a major factor. For infectious diseases, though, we are generally more interested in the extirpation of the agent rather than its preservation (Earn et al. 1998, Shea et al. 2000). Understanding the range of disease dynamics poses two challenges. First, we need to understand the relative and absolute importance of the regulatory (predator–prey-like interactions) and the stochastic forces (immigration probabilities and environmental and demographic stochasticity). The second challenge is to obtain reliable data, not only for large/dense populations, but also on small/sparse populations, for which data are difficult to obtain. We focus here on a microparasitic (viral) infection, where the pathogen reproduces in the host. Measles (and other human childhood diseases) provides a unique opportunity for understanding microparasitic dynamics, because it exhibits both endemic and episodic dynamics (Bartlett 1956), and because the data records are very good for both large and small host communities (Cliff et al. 1993, Bolker and Grenfell 1996, Grenfell and Harwood 1997, Keeling and Grenfell 1997, Grenfell and Bolker 1998). Large cities exhibit endemic cycles, while small towns exhibit recurrent epidemics interspersed with periods of local extinction.

The rich data base and cyclical dynamics of childhood infections have attracted the attention of nonlinear dynamicists interested in chaos and other nonlinear phenomena (Schwartz 1985, Olsen and Schaffer 1990, Sugihara et al. 1990, Rand and Wilson 1991, Mollison and Din 1993, Kendall et al. 1994, Ellner et al. 1995, 1998, Grenfell and Harwood 1997, Earn et al. 2000). This work has followed two directions, focusing respectively on mechanistic models and characterizing the nonlinear behavior of epidemiological time series. Recently, Ellner et al. (1998) integrated these approaches by developing ''semi-mechanistic'' time series modeling of the data. Finkenstädt and Grenfell (2000) extended this to a fully mechanistic time series model. Both these and other statistical approaches to the nonlinear dynamics of measles have focused on the endemic behavior of epidemics in large communities. Here we use a mechanistic model that allows us to explore the balance between noise and determinism across the full range of endemic and episodic measles dynamics. To achieve this synthesis, we develop a statistical SEIR (Susceptible–Exposed–Infectious–Recovered) model (the TSIR = the time series SIR [Susceptible–Infected–Recovered] model) that has a dual role. First, it is a model that can be scaled by population size to produce endemic and episodic dynamics (see Bartlett 1956). Second, it provides a mechanistic bridge between theoretical models and empirical data. We analyze a large spatiotemporal data set of measles incidence in England and Wales (Grenfell and Harwood 1997, Grenfell and Bolker 1998). In the present paper, we derive the model and show that it successfully represents the continuum from episodic to endemic dynamics, as we scale from small towns to large cities. The fitted model reveals a seasonally varying transmission rate, which closely corresponds to the seasonal aggregation of children at schools (Fine and Clarkson 1982*a*, Schenzle 1984, Finkenstädt and Grenfell 2000). We further obtain estimates of the scaling of infection rates—and thus reproductive ratios (R_0)—with host population size (De Jong et al. 1995). Finally, we use the model to explore the extinction/recolonization dynamics that drive the dynamics of measles in small places. In the companion paper (Grenfell et al. 2002), we show that this simple modeling framework for measles is capable of reproducing highly predictable fluctuations in large populations, and recurring episodic outbreaks in small populations. The dynamics in the large populations represents cyclic ''predator–prey'' dynamics involving the infected and susceptible individuals; the dynamics of the small populations resembles predator–prey metapopulations with predator outbreaks, host depletion, followed by predator extinction, host buildup, and recolonization (Grenfell and Harwood 1997).

We first summarize the relevant natural history of the microparasite (measles) and its host (humans), from which we develop the mechanistic model for the disease dynamics. We use the model first to understand endemic dynamics, where the deterministic component (the transmission process) is dominant. We subsequently scale the model down to investigate the episodic dynamics of small host communities for which demographic stochasticity and unpredictable recolonization events predominate (see Bartlett 1956).

Materials and Methods

Natural history and life cycle

The parasite.—Measles is caused by a highly infective single-stranded RNA virus belonging to the morbillivirus group (Barrett 1987). It may infect other primates, but is largely specialized on its human host. It is a classical microparasite (Anderson and May 1991), multiplying within the host with direct, mainly aerosol, transmission. Upon infection, the virus passes through

a latent period of ~6–9 d, followed by a 6–7 d infective period (Anderson and May 1991). The characteristic time scale of the transmission dynamics is thus ~2 wk. The infection results in either death or full recovery of the host. In immunocompetent and healthy individuals recovery is the norm, after which effectively a lifelong immunity to reinfection is acquired. Immunocompromised individuals may die following infection. In developing countries, measles is still a major cause of mortality (McLean and Anderson 1988). Case fatality in developed countries is very low (Anderson and May 1991). Thus, death due to disease is an unimportant factor in the time series we analyze here.

Due to its host specificity, measles dynamics resemble those of a simple two-species predator–prey system (Grenfell and Harwood 1997, but see Rohani et al. 1998). The high transmissibility and short infectious period of measles induce violent fluctuations in abundance, akin to predator–prey cycles (Anderson and May 1991, Grenfell and Harwood 1997). The cycles are driven by a rapid (initially roughly exponential) depletion of susceptible hosts through the course of an outbreak, and a subsequent slower (linear) buildup of susceptible through host reproduction and immigration (Bartlett 1956, Grenfell and Harwood 1997). The resultant tendency for cyclical dynamics is strengthened by seasonal variations in the infection rate.

In order for the virus not to go extinct, the replenishment rate of susceptibles must be quite high. Since birth numbers in humans depend on the number of adults in a community, there exists a critical community size (CCS) below which measles goes extinct during the epidemic troughs (Bartlett 1956, 1957, 1960*a*, Keeling and Grenfell 1997). The CCS appears to be ~300 000–500 000 in England and Wales in the prevaccination years. The dynamics in smaller communities depend to a great extent on repeated reintroduction of the virus into the host population through host movement (Bartlett 1956, 1960*a*, Grenfell and Harwood 1997, Keeling and Grenfell 1997).

The host.—Our aim in the following will be somewhat more modest than to review the population ecology, demography, and behavioral ecology (sociology) of the host of this particular morbillivirus. We will, instead, give a brief sketch of the important properties of the British people, as seen from the point of view of the single-strand of replicating RNA. We focus on the prevaccination era covered by the years 1944–1966.

Passive immunity to measles is passed from recovered mothers to their offspring via maternal antibodies. The passive immunity is lost after ~4 mo (Black 1984). Humans, thus, enter the susceptible host population after a short delay. Following this, the high transmission rates ensured that 95% of all people in (prevaccination) urban areas were infected by the age of 15, and essentially everybody by the age of 20 (Anderson 1982). In the prevaccination era, the mean age of infection was ~4–5 yr (Anderson and May 1991). Serological profiles showed a very conspicuous peak in infections at the age of school entry (Grenfell and Anderson 1985). Thus, birth rates and the behavior of children, most notably school children, largely determined the dynamics of measles.

The annual per capita birth rates of range from around 0.01 to 0.02 in Britain in the decades following World War II (Office of Population Censuses and Surveys; OPCS). The total production of susceptibles thus scaled with city size. However, the birth rates do vary geographically (Liverpool, for instance, has relatively high rates) and temporally (the post-World War II baby boom around 1947 resulted from a 30% increase in birth rates as compared to earlier and later periods; Grenfell et al. 1995, Finkenstädt et al. 1998, Finkenstädt and Grenfell 2000).

The core group for measles transmission was school-aged children. Aggregation during school terms therefore induced strong seasonal forcing in the transmission rates (Dietz 1976, Schenzle 1984, Grenfell et al. 1995). Cases invariably fell to a minimum towards the end of the summer holidays (a period during which the children were less aggregated), and rose thereafter to reach a peak in the early part of the calendar year (Fine and Clarkson 1982*a*, Anderson and May 1991, Finkenstädt and Grenfell 2000).

The final piece of the ecological jigsaw of measles infection is host movement: repeated outbreaks in small and rural areas require reintroduction of infection, generally from large population centers (Bartlett 1956, Cliff et al. 1993, Rhodes and Anderson 1996*a*, Grenfell and Harwood 1997, Grenfell and Bolker 1998). Bartlett (1960*a*, see also Murray and Cliff 1975) conjectured that the immigration rate of infected hosts scaled (but slower than linearly) with population size. Olsen et al. (1988) assumed the rate to be ~20 individuals/yr in a population of one million; however, this was mainly chosen to study aspects of the nonlinear dynamics of infection. Developing methods to estimate the spatial flux of infection from notification time series is a central aim of this paper.

The data

Cases of measles have been registered on a weekly basis by the UK Registrar General (OPCS). National notification was made mandatory in 1944 in England and Wales (Fine and Clarkson 1982*a*). The reporting is not complete during the period of mandatory notification. It is, however, rather good (reporting rate >50% in the prevaccination era; Clarkson and Fine 1985) and the underreporting can be corrected for through the process of susceptible reconstruction.

Mass vaccination started in 1968, after which the incidence of measles changed radically. The number of cases has been reduced from as much as 10 000 cases/wk in England and Wales to <100 cases/yr by the present (Grenfell and Harwood 1997). The change in incidence is followed by a shift in both temporal (Earn

et al. 2000) and spatial dynamics (Bolker and Grenfell 1996). After mass vaccination started in the early 1960s, susceptible dynamics are no longer governed by births alone. We, therefore, only consider prevaccination data spanning the time from 1944–1966 within this paper.

The records for >1000 urban and rural locations have been compiled (Grenfell and Bolker 1998). We analyze a subset of 60 cities spanning three orders of magnitude in population sizes, from 3.3×10^6 (London before the administrative creation of greater London) to 10 500 (Teignmouth). In 1965 ''greater London'' was created, with completely new (and much larger) political boundaries. (The birth rates and case counts reflect this change by a dramatic increase for ''London'' thereafter.) In consequence, we only consider the London data up until the end of 1964.

Along with the number of infected cases, the other key state variable is the number of susceptibles (Anderson and May 1991). Susceptibles are depleted through epidemics, but replenished by host reproduction. We have, therefore, compiled the relevant birth rates and number of births for each of the cities through the years in question (Finkenstädt and Grenfell 1998, Finkenstädt et al. 1998). The births themselves do not represent a measure of the number of susceptibles, but the records allow us to generate time series of susceptibles through standard susceptible reconstruction algorithms (Fine and Clarkson 1982*a*, Schenzle 1984, Ellner et al. 1998, Bobashev et al. 2000, Finkenstädt and Grenfell 2000). In principle, this can be achieved without explicitly considering birth rates (Bobashev et al. 2001). However, we shall subsequently want to simulate the epidemiological effects of changes in birth rate. We, therefore, carry out susceptible reconstruction using the algorithm proposed by Finkenstädt and Grenfell (2000). In summary, this method reconstructs the dynamics of the unobserved susceptible class from data on births and reported cases. The size of the susceptible class reflects a balance between the rate of loss of passive maternal immunity of infants (assumed to occur at 4 mo) and the recovery rate of recently infected individuals (who have active immunity henceforth). The susceptible reconstruction is achieved by regressing cumulative births against cumulative case notifications (see Finkenstädt and Grenfell 2000 for details). The residuals from this regression represent the cyclical deviation of the susceptible class around the mean number of susceptibles, S, as driven by the epidemic dynamics. We denote the deviations by z_t. The only assumption necessary to make for this to work is that the reporting rate is constant through time. Since the 1944–1966 period showed significant changes in public health and socioeconomic patterns, it makes sense to allow for the possibility of smooth changes in reporting rates. We do this by using a locally linear regression of the cumulative–cumulative plot (Finkenstädt and Grenfell 2000). Cross-validation is used to optimize the bandwidth of the locally linear regression (Finkenstädt and Grenfell 2000). There is a valuable spinoff of susceptible reconstruction for extremely contagious diseases, like measles, in developed countries during the prevaccination era. In such cases, it is reasonable to assume that the number of individuals that die without having contracted the disease is negligible. Thus, the slope of the (global or local) cumulative–cumulative regression is a direct reflection of the reporting rate. We use the estimated reporting rate (of just over 50%); to calibrate the case counts. Note that susceptible reconstruction will be less reliable in the earliest part of the time series. A corollary to this is that ''initial conditions'' are harder to estimate if no allowance is made at the beginning of the series. A further potential problem for susceptible reconstruction would be variations in reporting rate with infection level (and therefore across the epidemic cycle; however, this does not seem to be a major issue for measles (Clarkson and Fine 1985).

The raw data for the 60 cities—the biweekly incidences of measles and the annual data on human birth rates—are available from the Department of Zoology at Cambridge University.[5]

The model

A stochastic disease model.—The SEIR (Susceptible–Exposed–Infectious–Recovered) class of models is a cornerstone of ecological epidemiology, as it provides a simple mechanistic model for microparasite dynamics. In the theoretical literature, deterministic continuous-time, continuous-state-space formulations are the most common (e.g., Schenzle 1984, Anderson and May 1991, Grenfell and Dobson 1995, Earn et al. 2000). We will, however, extend the discrete-time model of Finkenstädt and Grenfell (2000) to formulate a discrete state-space model that can accommodate small population sizes and disease recolonization.

The natural time scale for the disease is ~2 wk. We therefore aggregate the weekly data into 2-wk intervals, and use this as the time step in the model. The time series for each of the 60 cities contains 598 two-week intervals for the years 1944 through 1966.

We denote the number of resident infectious host at time t ($t = 1, \ldots, T$) by I_t, and the number of immigrant infections by θ_t. The force of infection, that is the infection pressure experienced by one susceptible individual, is then given by $\beta_s(I_t + \theta_t)^\alpha$, where β_s is the transmission rate. Here, the transmission rate is allowed to vary through time with a 1-yr period to accommodate the seasonal cycle of school terms (Fine and Clarkson 1982*a*, Grenfell et al. 1995, Earn et al. 2000). The parameter α allows for the nonlinearities in contact rates that may arise due to spatial substructuring or other forms of nonhomogenous mixing (Fine and

[5] URL: ⟨http://www.zoo.cam.ac.uk/zoostaff/grenfell/measles.htm⟩

Clarkson 1982*a*, Liu et al. 1986, 1987). Mass action corresponds to $\alpha = 1$. Mixing effects can also result in the susceptible, S_t ($=\bar{S} + z_t$), entering the transmission equation in a nonlinear fashion. The overall epidemic intensity is thus given by

$$\lambda_{t+1} = \beta_s (I_t + \theta_t)^{\alpha} (\bar{S} + z_t)^{\gamma} \quad (1)$$

where γ allows for the further nonlinearities in transmission. A way of conceptualizing α and γ is to think of schools as the hot spots for transmission of measles. Whenever transmission among pupils that belong to the same school classes (and within schools) is, on average, greater than that between children of different schools, the result is spatial substructuring between the susceptible and infective class. This can, from a citywide perspective, lead to mixing coefficients that are lower than unity. If the spatial component of transmission dynamics were to be ''symmetrical,'' in the sense of infected individuals being equally clustered in the increase phase of the epidemic as susceptibles are in during the decline phase, then α and γ should be identical. At a slightly more phenomenological level, $\alpha < 1$ may also be seen as a conversion factor when going from continuous to discrete time (K. Glass and B. T. Grenfell, *unpublished manuscript*; see *Discussion*). However, since $\bar{S}$ is not easily identifiable when γ is unknown, we will set γ equal to one during the estimation. We revisit this assumption in the discussion.

The epidemic intensity is never realized exactly in a finite population because of the discreteness of individuals and demographic stochasticity. The demographic stochasticity that arises from an epidemic birth–death process has been studied intensively (Kendall 1949, Bartlett 1956, 1960*b*). If we assume that the rates of the process are approximately the same through the 2-wk interval, then the number of secondary cases from a single infected individual will be geometrically distributed (e.g., Kendall 1949). Starting with I_t infected individuals, and assuming independence between them, the birth–death process will hence be realized according to a negative binomial distribution (Kendall 1949, Bartlett 1956, see also Renshaw 1991)

$$I_{t-1} \sim \text{NB}(\lambda_{t+1}, I_t) \quad (2)$$

where, NB(a, b) signifies a negative binomial process, with expectation a and clumping parameter b. Note, that this formulation is closely linked to the chain-binomial model (Bailey 1957), but has the advantage that its relation to the SEIR model is direct. It has the additional advantage over the chain-binomial model that it can be estimated with data from susceptible reconstruction.

We assume that the disease migration rate is an independent stochastic process. Migration rates of the disease are believed to be quite low even in large cities, and then to scale with population size (Bartlett 1960*a*). As a simplification we will assume that within a 2-wk window, the number of immigrant infections is

$$\theta_t \sim \text{Poisson}(m) \quad (3)$$

where m is a time-invariant immigration intensity. The TSIR model (Eqs. 1–3) for the disease dynamics is thus a doubly stochastic model.

The susceptible dynamics are governed by

$$S_{t+1} = S_t + B_t - I_{t+1} \quad (4)$$

where B_t is the number of births into the host population during the 2-wk interval t. This number varies through time (see *Materials and methods: Natural history and life cycle: The host*).

We will, for now, ignore any additional environmental stochasticity in the disease dynamics. Eqs. 1–4, thus, provide a simplified, yet fully specified, stochastic model for the dynamics of measles that can represent both small and large cities. There are two snags to parameter estimation and statistical inference.

Estimation.—Eqs. 1–3 provide a fully specified statistical model for the parameters whenever records for $\{I_t; t = 1 \ldots T\}$ and $\{S_t; t = 1 \ldots T\}$ exist. The model equations represent a non-Gaussian, nonlinear, hierarchical model for abundance data (e.g., Bjørnstad et al. 1999). We outline the estimation framework in Appendix A and Appendix B. Note though that we are still working to improve this framework (Finkenstädt et al. 2002). The seasonal transmission coefficients, β_s, are modeled as the most general sequence of transmission rates that is ensured to have a period of 1 yr, by allowing a unique parameter for each of the 26 two-week periods of the year (which is repeated across all years; Finkenstädt and Grenfell 2000). The immigration process is an unobserved stochastic process. In the absence of underreporting, the immigration intensity can be estimated using Markov chain Monte Carlo methods. However, the estimator of the mean immigration intensity, $\hat{m}$, will be biased upwards in the presence of measurement error (see Appendix B). The current results have been obtained using the moment expansion of Eq. 1 (see Appendix B):

$$\log(\lambda_{t+1}) \approx \log \beta_s + \alpha \log I_t + \frac{\alpha m}{I_t} + \log(\bar{S} + z_t). \quad (5)$$

Notice that we have set γ to 1, so that we can uniquely estimate the mean number of susceptibles, $\bar{S}$. As detailed in Appendix B, we estimate $\bar{S}$ marginally on all the other parameters (using profile likelihood; e.g., Hilborn and Mangel 1997). The α and the seasonal β parameters, a total of 27 parameters, are estimated conditionally on $\bar{S}$, but marginally on m, using standard linear likelihoods. Finally, we estimate m using a somewhat ad hoc nonlinear minimization (see Appendix B). For each of the 60 time series we thus estimate 29 parameters on the basis of 597 observations. For all

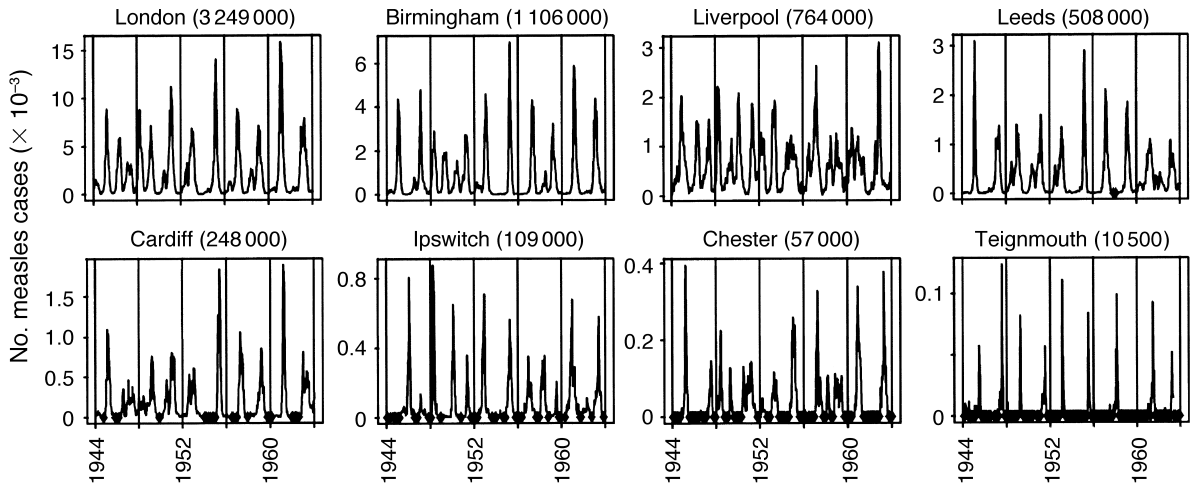

FIG. 1. Biweekly counts (in thousands) of measles cases from 1944–1964 for eight cities in England and Wales. The numbers have been corrected for underreporting (mean reporting rate = 52%). The cities are arranged by size. The three first panels (top) represent the three biggest cities in England and Wales (London, Birmingham, Liverpool). The five subsequent panels show a range of city size down to Teignmouth with 10 500 inhabitants. Black dots along the *x*-axis represent zero counts. City names (and populations) are given above the panels. The *y*-axis numbers are in thousands of cases.

but one of these (*m*), one-step-ahead prediction (viz. conditional least squares) is used for estimation. If this seems like a large number of parameters, we ask the reader to keep in mind that there are >20 observations per parameter, and that there are >35 000 observations in the full spatiotemporal data panel. Note also that we do not use truly independent data sets to assess model fit—rather we use the unusually high consistency across different cities, and what effectively amounts to a meta-analysis of independent data sets, to vouch for the generality of the results. Judicious smoothing would easily reduce the number of seasonal parameters; however, we leave that as a task for the future.

Since periods of local extinction do not contain information about α, β_s, and $\bar{S}$, we omit these data points during the likelihood estimation (Eq. 5). The whole time series is used to estimate *m*.

Scaling of rates and parameters.—Several of the parameters may be expected to scale with city size (Anderson and May 1991). The mean number of susceptibles is the most obvious, as it depends directly on population size. The relative importance of the demographic stochasticity is likely to decrease with population size; since $\lambda_{t+1} \approx I_t$ for the measles epidemic, the coefficient of variation (CV) of the negative binomial process (see, for example, Evans et al. 1993) given by Eq. 2 is approximately equal to $\sqrt{2/I_t}$. Note, thus, that the CV changes through the epidemic cycle. The population-level immigration rate may be expected to increase with host community size, since smaller cities have a lower number of potential ''migrants''. The relative importance of spatial (metapopulation) dynamics vs. local regulatory (transmission) dynamics is likely to be higher in small populations. The transmission coefficients, β, may scale with population size depending on whether the dynamics adhere to frequency dependent transmission (''true mass action'': $\lambda = \beta IS/N$, where *N* is the host community size) or density dependent transmission (''pseudo mass action'': $\lambda = \beta IS$; De Jong et al. 1995, McCallum et al. 2001). Whether the mixing coefficient, α, differs between small and large host communities, is an open question.

RESULTS

The time series of biweekly counts for eight of the 60 populations are depicted in Fig. 1. These eight cities represent the three largest cities in the England and Wales data set and a range across other city sizes. The selection spans the range from London (with $>3 \times 10^6$ inhabitants prior to the agglomeration into Greater London in 1965) to Teignmouth (with 10 000 inhabitants in 1960). The large cities exhibit fairly regular, generally biennial, endemic disease cycles with few or no fadeouts. Cities in the range 50 000 to ~300 000 inhabitants exhibit occasional and brief fadeouts. The smallest communities exhibit long fadeouts and irregular outbreaks. The transition in dynamics is reflected in the mean number of biweekly cases and the fraction of zero observations in the (biweekly) time series (Fig. 2). The mean case count rises linearly with city size (Pearson correlation = 0.996, $P < 0.01$). The proportion of zeros declines exponentially up to a critical community size, after which no zeros are recorded (Spearman rank correlation = −0.91, $P < 0.01$; see also Bartlett 1960*a*).

Susceptible reconstruction reveals a mean reporting rate of just over 52% (SE = 0.01), ranging from as low as 30% and as high as 65%. This accords with previously reported values (Clarkson and Fine 1985, Finkenstädt and Grenfell 2000). There is no relation be-

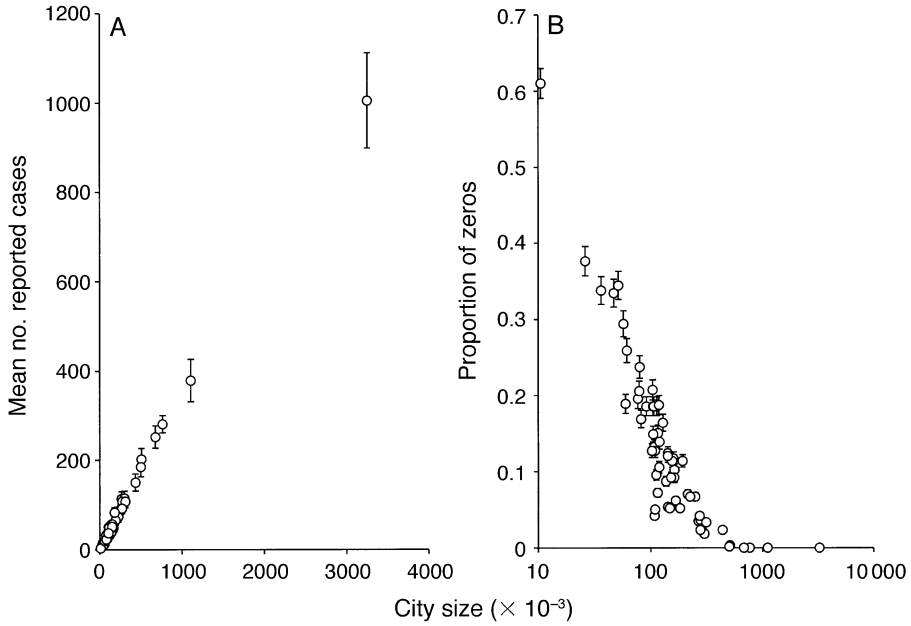

FIG. 2. (A) Mean number (across 1944–1967) of biweekly cases reported (not corrected for underreporting) against city size (in thousands) for the 60 cities. The error bars represents twice the ''naive'' standard errors (calculated assuming independence of observations; true errors are likely to be wider). (B) The proportion of the biweekly time series that are zeros (across 1944–1967) plotted against city size in thousands (on a log scale). The error bars represent twice the ''naive'' standard errors for the proportion (calculated assuming independence of observations). The critical community size, above which no fadeouts occurs, is ~300 000–500 000.

tween the reporting rate and city size (Spearman rank correlation $= -0.04$, $P = 0.73$).

The correlation between observed and predicted is generally very good (Fig. 3). The mean R^2 (here measured as 1 − [residual deviance/null deviance]) for the 60 fitted models is 0.85. The model fit scales directly with population size from Teignmouth ($R^2 = 0.74$) to London ($R^2 = 0.98$). The Spearman rank correlation between the R^2 and the population size is 0.92. This indicates that the short-term predictability of the dynamics increases with population size.

The estimated mean number of susceptibles is proportional to the community size (Pearson correlation $= 0.998$, $P < 0.01$), so that the fraction of susceptibles appears to be constant around 3.2% (SE = 0.05; Fig. 4). Through an epidemic cycle, the proportion of the population that is infected and susceptible appears to be independent of population size (Fig. 5). The proportions typically span 0% to ~0.3% (with a mean of 0.06%) in the former and 2.1% to ~4.2% in the latter. This is a smaller proportion susceptible than is generally estimated for measles in developed countries (Anderson and May 1991). We will return to this discrepancy in the discussion.

Transmission

The estimated mixing parameter, α, is very close to unity; The mixing between infected and susceptibles is therefore close to homogenous. The weighted mean (weighted, as in a meta-analysis, by the reciprocal of the variance of the estimates) across the 60 cities is 1.006 (SE = 0.004). There is weak evidence that α decreases with community size (weighted Pearson correlation $\rho = 0.28$, $P = 0.03$). However, the change appears to be ecologically unimportant (Fig. 6).

The transmission parameters, β_s, are both a function of season and of community size. The annual mean transmission parameter scales inversely with log(community size) according to (weighted regression: $R^2 = 0.95$, $P < 0.01$; Fig. 7)

$$\log(\bar{\beta}) = 3.64[\pm 0.39] - 1.02[\pm 0.03] \times \log N \quad (6)$$

where N is the community size. There is, however, significant seasonal variation ($P < 0.01$ for all 60 cities). Fig. 7b shows the seasonal deviation around the mean log-transmission rate of each city. The figure represents the (weighted) mean across all the 60 cities. The signature of school-term aggregation is apparent in that the realized transmission rates are low during school holidays. The pattern appears, however, to be more complex than a simple on/off situation (Finkenstädt and Grenfell 2000, see also Fine and Clarkson 1982*a*). Note that reporting is often delayed before the New Year; the estimates during the first and last biweek of the year are therefore less accurate, and are likely to be biased.

The reproductive ratio, R_0, is the expected number of secondary cases resulting from one infected individual in a community where all individuals are susceptible: $R_0 = \beta N^{\gamma}$. We cannot estimate R_0 directly

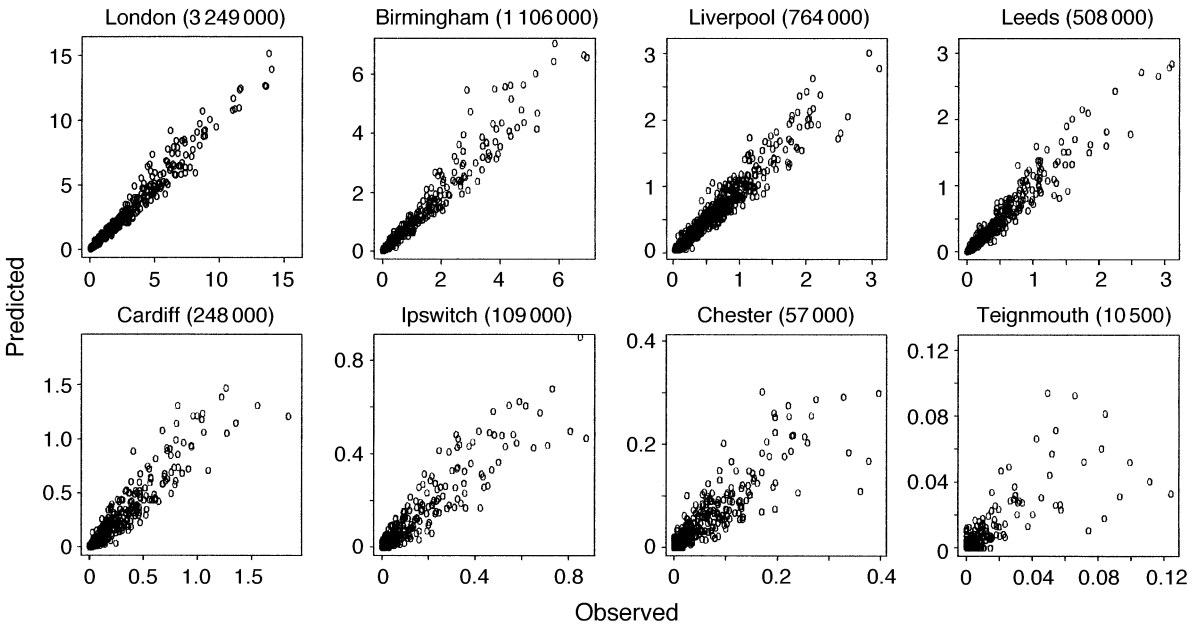

FIG. 3. The predicted vs. observed values for the TSIR model for the eight cities depicted in Fig. 1. The R^2 values (on a log scale, measured as 1 − [residual deviance/null deviance]) are 0.98 (London), 0.96 (Birmingham), 0.92 (Liverpool), 0.95 (Leeds), 0.89 (Cardiff), 0.84 (Ipswitch), 0.79 (Chester), and 0.74 (Teignmouth), respectively. Note that the model fit is assessed on a log scale, since that is the natural scale for estimation (Eq. 5). City names and populations are given above the panels. The *y*-axis numbers are in thousands of cases.

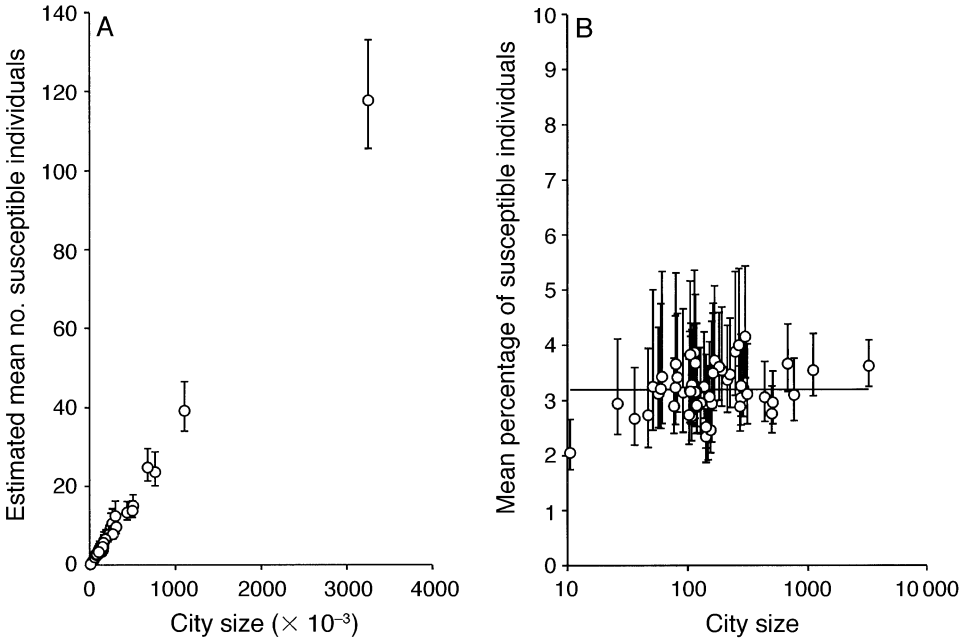

FIG. 4. (A) The estimated mean numbers of susceptible individuals (in thousands) against city size (in thousands). Error bars represent 95% confidence intervals as determined from likelihood profiles. (B) The same estimates as in (A), but represented as a percentage of the city size. Note that the *x*-axis is on a log scale. The horizontal line represents the grand mean at 3.2%. The *y*-axis numbers are in thousands of cases; the *x*-axis numbers are in thousands of individuals.

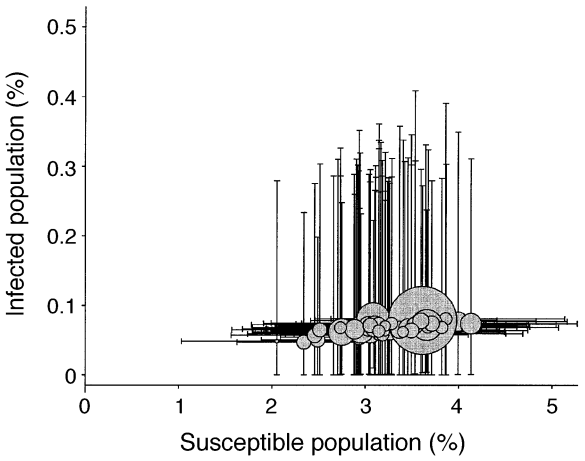

FIG. 5. The percentages of the populations that are infected (*y*-axis) and susceptible (*x*-axis). Dots represent the mean of each population. The sizes of the dots are proportional to the city size. The horizontal bars represent the upper and the lower fifth percentile in proportion susceptible. The vertical bars represent the upper and the lower fifth percentile in proportion infected.

without knowing both mixing rates, α and γ, of Eq. 1. We can, however, estimate how the R_0 varies as a function of population size. If we compare the R_0s of all the 60 cities relative to the mean ratio for London, there appears to be no relationship between R_0 and population size (Fig. 8). Since the transmission rate varies seasonally (Fig. 7), the actual R_0 will depend somewhat on when in the seasonal cycle the infection is introduced. During the biweek of lowest transmission rate (late August), the relative R_0 is only 66.2% (SE = 2.0%) of the annual mean. Late December, in contrast, has a relative R_0 of 130.7% (SE = 4.0%). We discuss the absolute levels of the R_0 in the *Discussion.*

Colonization and immigration

We found the biweekly immigration rate to scale with population size. For the smallest community (Teignmouth; population 10 000) it is ~0.2 (95% CI = 0.14, 0.27). In expectation, this yields less than one immigrant event about every 3 mo. Communities of ~100 000 have a biweekly rate of about unity. Gateshead (population 111 000), for instance, has an estimated rate of 0.96 (95% CI = 0.77, 1.37), an immigration event slightly more frequently than once a month. Cities around the critical community size (population 300 000), have an estimated rate around four. The confidence intervals are, however, huge for bigger cities; Liverpool (population 764 000), for instance, has an estimated rate of 2.9, that may be as low as 2.0 and as high as 20. The wide confidence intervals in big cities reflect how their dynamic trajectories provide relatively small amounts of information about the immigration process. The estimated migration rate scales roughly with the square root of the population size (Pearson correlation 0.91, $P < 0.01$). Note, though, that important issues remain unresolved with respect to estimating coupling; B. Finkenstädt, O. N. Bjørnstad, and B. T. Grenfell, *unpublished manuscript,* use detailed statistical simulation to show that the relationship between immigration rate and population size may be spurious. Bias in this parameter, fortunately, does not affect the other estimates (see Appendix B).

An immigration event will not always spark off an epidemic in a community where measles has faded out. The chance of sparking off an epidemic given one immigrant is determined according to a geometric distribution with parameter $\beta_s(\bar{S} + z_t)$ (see *Materials and methods: The model: A stochastic disease model*). This parameter depends on the number of susceptibles, which is relatively low in the initial phase of the fade-out period (typically ~2% of the population) and rises as susceptibles build up through host reproduction (to ~4–5%). Looking at the smallest city, Teignmouth (population 10 000) with an estimated minimum number of susceptibles of 68 and a maximum of 383, the odds of sparking off an epidemic is <1:5 with the low number, and about 1:1 with the high number (using the mean β-value). The odds are about 1:2 for the mean number of susceptibles (= 216). The odds of sparking off an epidemic from one immigrant for mean, low, and high numbers of susceptibles is relatively invariant across all the 60 populations at 1:1, 1:2, and 3:2.

More generally, the probability of stimulating an epidemic from θ immigrants, is given by $1 - (1 + \lambda/\theta)^{\theta}$, where λ is as defined in Eq. 1. Scaling mean transmission rates according to Eq. 6, we can tabulate the odds of sparking off an epidemic from one and two immigrants across a range of city sizes below the CCS (Fig. 9a). The odds are governed by the proportion of

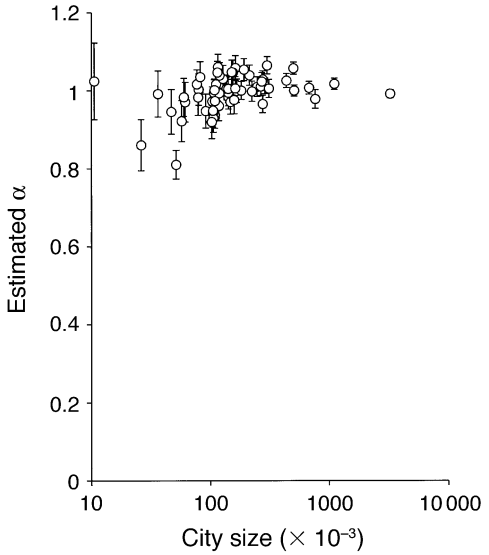

FIG. 6. The estimated mixing coefficient, α, plotted against city size in thousands (on a log scale). The *x*-axis numbers are in thousands of individuals.

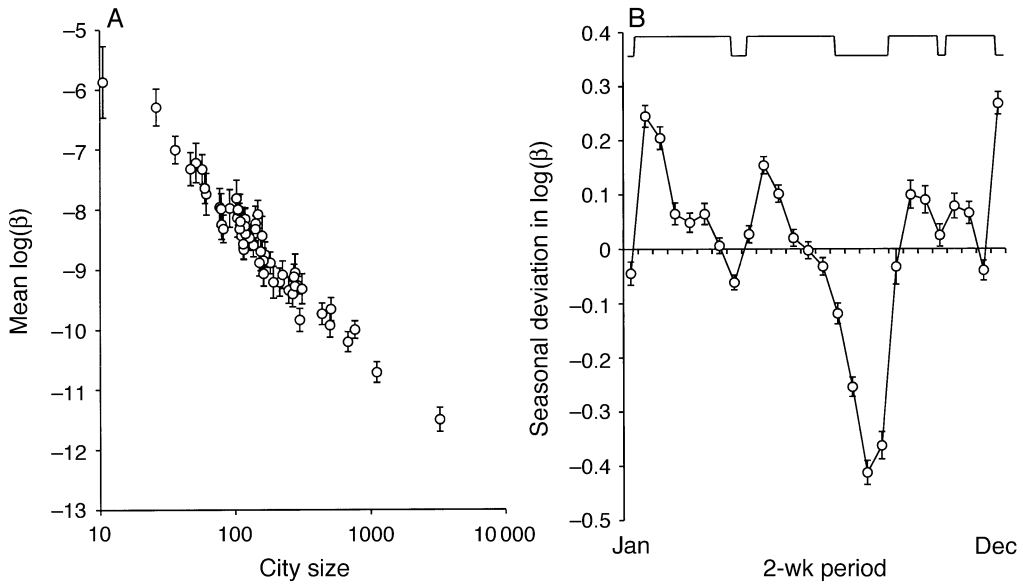

FIG. 7. The estimated transmission rates. (A) The mean (across the seasonal cycle) transmission rate, β (on a log scale), plotted against city size in thousands (on a log scale). The error bars represent the across-year standard deviation around the mean. The *x*-axis numbers are in thousands of individuals. (B) The seasonal deviation (by 2-wk interval) around the mean transmission rate. Estimates represent weighted means across the 60 cities. The error bars represent 1 SE around the mean. The curve along the top shows school terms (high level) vs. major holidays (low levels) through the year (Fine and Clarkson 1982*a*).

susceptibles; thus, when that proportion is relatively invariant across the populations, the odds will be fairly invariant. With proportions ranging from ~2% to just over 4%, the odds are predicted to vary from 1:2 to just over 1:1 with one immigration event, and from just over 1:1 to ~4:1 with two (Fig. 9a).

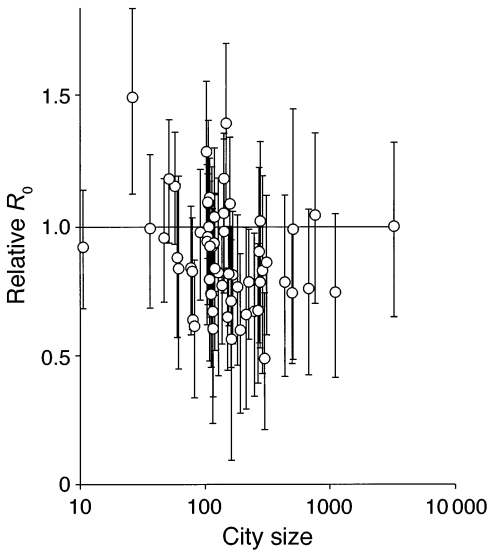

FIG. 8. The relative basic reproductive ratio for the 60 cities, against city size in thousands (on a log scale). The ratios have been scaled according to the mean in the largest city (London). The circles represent estimates based on seasonally averaged transmission rates. The vertical bars represent the relative R_0 for the 2-wk period of lowest and highest transmission rates (see Fig. 7). The *x*-axis numbers are in thousands of individuals.

Once an epidemic has started, the influence of any additional immigrants is small. In fact, the relative influence of an immigrant in the subsequent growth of the epidemic drops geometrically with the number of local infecteds. (We here measure ''relative influence'' as the proportionate difference in the epidemic growth from both local and immigrant infection relative to that expected solely from local contagion.) An immigrant will have <5% influence on the growth rate as soon as there are more than about five resident infected individuals. By ~20 resident infecteds the influence is >1%. The relative influence of immigrants is tabulated in Fig. 9b. Among the 60 cities, the influence of an individual immigrant is <10% all but 0–10% of the time in the cities with populations >500 000. This explains why there is so little information pertaining to the migration process in large cities, and why the confidence intervals for *m* are so wide. For cities with populations between 200 000 and 500 000, the influence is <10% for ~80% of the time. Even for the very smallest cities (population <50 000), the influence is negligible as soon as the epidemic has flared up and is past a few resident infecteds (Fig. 9b). These results, together with the $\sqrt{2/I}$-scaling of the CV of the demographic stochasticity (see *Materials and methods: The model: Scaling of rates and parameters*), indicate that there is a threshold shortly after epidemic take off where the dynamics are approximately ''deterministic'' (in all but the smallest communities; see Grenfell et al. 2002).

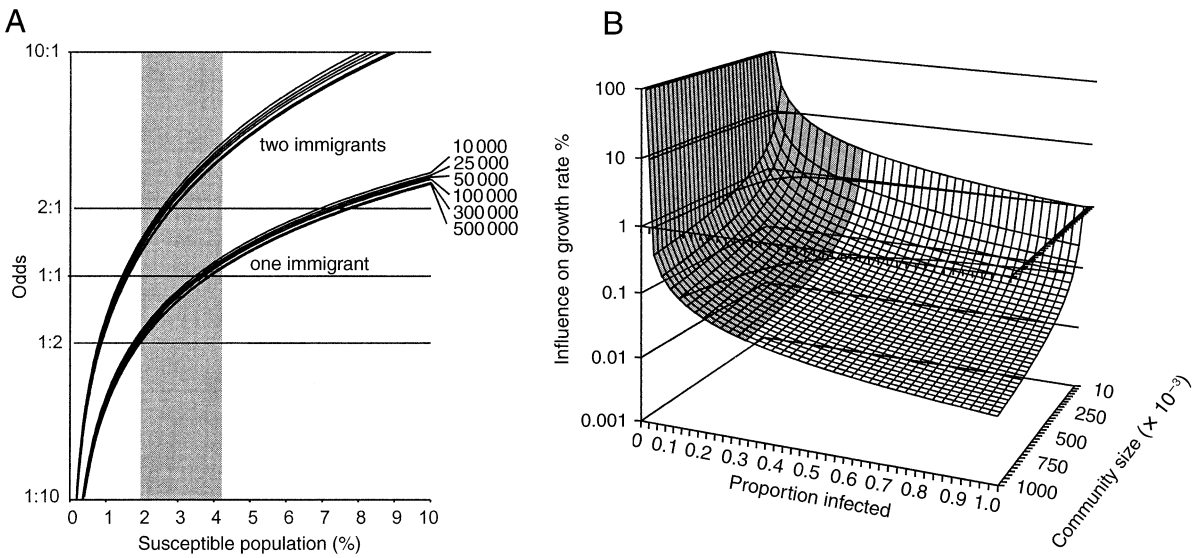

FIG. 9. (A) The odds (on a log scale) of sparking off a new epidemic plotted against percentage of the population that is susceptible given one immigrant (lower lines) or two immigrants (higher lines). The odds are relatively invariant across community size (the cluster of lines represents six different community sizes below the CCS. The grey-shaded area represents the range in susceptible proportions observed in the data. (B) The influence of one immigrant on the disease dynamics (as a percentage of the growth rate; on a log scale) as a function of the proportion of resident individuals that are infected and the size of the host community.

DISCUSSION

The dynamics of measles have played a key role in theoretical epidemiology (Bartlett 1957, 1960*a*, Fine and Clarkson 1982*a*, Schenzle 1984, Olsen and Schaffer 1990, Sugihara and May 1990, Anderson and May 1991, Grenfell 1992, Bolker and Grenfell 1993, 1996, Mollison and Din 1993, Kendall et al. 1994, Ellner et al. 1995, 1998, Rhodes and Anderson 1996*b*, Keeling and Grenfell 1997). This work parallels the development of several ideas in ecological population dynamics (intrinsic density dependence vs. extrinsic forcing, deterministic vs. stochastic dynamics, spatial coupling and synchrony, etc.), though we would argue that measles provides a less cluttered path between data and mechanistic models than most other systems. Childhood infections have also been a key test bed for understanding dynamical systems and associated statistical methodologies at the population level (Schaffer and Kot 1985, Sugihara et al. 1990, Casdagli 1991, Rand and Wilson 1991, Stone 1992, Drepper et al. 1994, Grenfell et al. 1994, Stone et al. 1996, Finkenstädt and Grenfell 2000). In this paper, we presented a modeling framework that weds the theoretical and statistical approaches through a mechanistic, stochastic model for measles epidemics (see also Finkenstädt and Grenfell 2000). We subsequently developed and applied an estimation framework to quantify the parameters of the model. We fitted the model to data from 60 cities from England and Wales exhibiting the range from endemic disease cycles (''Type 1 dynamics'' sensu Bartlett 1957) to irregular episodic outbreaks (''Type 3 dynamics''). In the companion paper (Grenfell et al. 2002), we show that the model is able to describe and regenerate the quantitative and qualitative properties of the different types of dynamics in these 60 cities. In the current paper we have focused on how the dynamic rates scale with host community size, and their associated implications for the ecology of the infectious disease. An overarching finding is that certain parameters scale in a simple fashion across three orders of magnitude of host population sizes. Other parameters/descriptors are fully invariant across the same range. The case count, for instance, scales linearly with city size (Fig. 2). This scaling is, however, not surprising since it is well known that essentially all children were infected with the virus in the prevaccination era (Anderson 1982).

Mixing, transmission, and R_0

The mixing parameter (α) is found to be nearly independent of host community size and very close to unity (Fig. 6). This indicates that the transmission dynamics are close to homogenous mixing. Note, though, that analyses presented by Finkenstädt and Grenfell (2000) suggest that α is slightly lower than unity (see *Discussion: Discrete time modeling*). The seasonal pattern of disease transmission is also similar across the range of host population sizes (Fig. 7b). This pattern is a fair reflection of the annual cycle of aggregation among school children. Periods of low transmission coincide with school holidays (see *Discussion: Implicit age structure*).

In contrast to the seasonal pattern of transmission, the mean transmission rate ($\bar{\beta}$) scales tightly with host

community size. Log($\bar{\beta}$), is inversely proportional to log(size) (Fig. 7a). This scaling is consistent with frequency dependent transmission (true mass action, the force of infection is determined by $\beta I/N$) rather than density dependent transmission (pseudo mass action, the force of infection is given by βI; De Jong et al. 1995, McCallum et al. 2001). Frequency-dependent transmission occurs where the local spatial density of ''transmissive'' contacts between susceptible and infectious individuals is independent of population size (Diekmann et al. 1996, Begon et al. 1998, 1999, Swinton et al. 2002). Viewed in this context, our results suggest at first glance an ''urban population density'' common across small towns and large cities. Generally, this flies in the face of intuition about human diseases, since we would expect a markedly higher density of contacts in large cities, especially if we take into account local stochastic ''gaps'' in transmission in small towns. (An important illustration of this latter epidemiological effect of population density was provided by Anderson and May [1991], who analyzed the dynamics of smallpox eradication. Regions with a higher density of susceptibles required higher vaccine uptake rates for local disease extirpation testifying to increased transmission rates.) However, for measles, the scaling of $\bar{\beta}$ with population size is likely to arise because the effective density of the core group, children in school classes and their epidemiologically coupled preschool sibs, vary much less with urban population size than the overall density of adult contacts. Thus, social organization appears to render the density and size of the core group for disease transmission remarkably invariant. There is much scope for refining the TSIR approach here, particularly in examining the scaling of infection rate across a wider range of urban and rural densities and analyzing the impact of cross-cultural variations in family size and schooling patterns on disease transmission (Black 1984, Anderson and May 1991, Cliff et al. 1993, Grenfell and Bolker 1998).

One consequence of the scaling in transmission rates is that the mean force of infection (mean across season) is independent of host population size at 0.019 (SE $<$ 0.001). The basic reproductive ratio, R_0, is similarly relatively independent of population size (Fig. 8).

The exact value of R_0 can only be estimated if all mixing coefficients are known. If we assume mixing to be homogenous, the R_0 that would correspond to the mean transmission rate is 29.9 (SE = 0.9) and over the seasonal cycle it would change from a minimum of 19.8 (SE = 0.6) in August to a maximum of 39.1 (SE = 1.2) in December. These estimates are significantly higher than the standard estimates of ~14–18 (Anderson and May 1991). There are two possible biases in our estimate. First, if the mixing rate, γ, is smaller than unity, then the R_0 from the TSIR model will be lower than numbers calculated. Second, the R_0 will be lower if the characteristic time scale is somewhat shorter than 14 d (see *Discussion: Discrete time modeling*).

The mean number of susceptibles is found to be directly proportional to the community size (Fig. 4). So much so, that the mean proportion of susceptibles appears invariant at ~3% of the host population. Epidemiological theory (see Anderson and May 1991) predicts that the mean proportion of hosts susceptible to a microparasite governed by simple SIR dynamics is inversely related to R_0. As a conjecture to more complicated (seasonally forced) dynamics, this seems to work for the current data set. Applying $N/\bar{S}$ as a crude estimator, R_0 is predicted to be invariant of population size at 31.9 (SE = 0.6). Note, though, that a mean susceptible proportion of 3% is significantly lower than the 9% level concluded by Fine and Clarkson (1982*b*). The discrepancy may be due to a number of factors; a possible candidate is the collapsing of the age structure implicit in the model (Earn et al. 2000). Second, the problem could also arise from our assumption that the ''mixing'' parameter on susceptible density (γ in Eq. 1) is unity. Finally, as is the case for R_0, the estimate of $\bar{S}$ depends partly on the characteristic time scale assumed. We explore this dependence below (see *Discussion: Discrete time modeling*).

Migration and coupling

The disease immigration rate is estimated to scale with population size. As conjectured by Bartlett (1960*a*), the immigration rate appears to scale slower than linearly with population size. The pattern must be viewed with caution, however, since Finkenstädt et al. (2002) show that the relationship between immigration rate and population size may partly be an artifact of differential bias in small vs. large cities.

The odds of sparking off an epidemic (given one immigrant and prior disease extinction) appears to be relatively invariant to population size (Fig. 9a). This seems to come about through balancing of the transmission parameter against the mean number of susceptibles, so that the proportion of susceptibles remains between 2% and just over 4%. Grenfell and Harwood (1997), Grenfell and Bolker (1998), and Grenfell et al. (2001) discuss the metapopulation dynamics of measles. The fact that the susceptible population size never grows (through host reproduction) much above where the odds of sparking off an epidemic are even, indicates that the regulation through metapopulation dynamics is rather efficient. Upon growing above a certain size, the disease quickly ''catches fire'' to deplete the susceptible population size.

The influence of immigration is of little importance in big cities (Fig. 9b), and even for small cities immigration is only important at the onset of epidemics. Once the epidemic gains momentum additional immigrants have little influence on the course of the trajectory. Thus, both the stochasticity due to the immigration process as well as the stochasticity inherent in the birth–death process decrease fairly rapidly with community size and epidemic size. Above some thresh-

old, we can thus think of the fate of the epidemic as deterministic (in all but the smallest communities; Grenfell and Harwood 1997).

In the model, we assumed time independence of the immigration intensity. This is likely to be overly simplified because the dynamics of measles in England and Wales are highly synchronized between cities (Bolker and Grenfell 1996, Grenfell et al. 2001). The result is a country-wide pool of infecteds that varies greatly through time. The true immigration intensity is likely to vary as a function of changing donor population size, and the pattern of coupling between cities. We are currently working to understand better the coupling in disease dynamics (Grenfell et al. 2001). A consequence of time-varying immigration intensities will be that the recolonization process will be more predictable than assumed in our model (Eqs. 1–4). ''Immigration'' of infection to a town may in fact occur by direct movement of nonresident infected individuals or via temporary excursions by local susceptible individuals. In our current model formulation, we treat these as synonymous. Teasing out any differences arising from these two modes of spatial transmission is an important area for future work.

Implicit age structure

The transmission rate of measles is known to be age structured (Fine and Clarkson 1982*b*, Schenzle 1984, Grenfell and Anderson 1985, Anderson and May 1991, Grenfell 1992). The contact rate is highest among school children, because the schools represent a demographic hot spot for mixing between infecteds and susceptibles. School-related aggregation of children induces a strong seasonal forcing on the transmission rates as evidenced in the data (Fig. 7b, see also Finkenstädt and Grenfell 2000). The correspondence between the estimated transmission rates and the term time is, however, less than perfect. While the school aggregation is an on/off process, the seasonal transition changes more gradually. The transmission rates are generally lower during school holidays than during term, and the transmission rates peak in the beginning of school term. However, the transmission appears to drop gradually through the term. A probable reason for this lies in the age structure; high risk (i.e., high contact) individuals are removed from the susceptible population at a higher rate than low risk individuals. The mean (realized) contact rates will therefore drop with time. (Such effects of heterogeneity are well known in statistical demography; see for example, Vaupel et al. 1979, Keyfitz and Littman 1980, Vaupel and Yashin 1985). In line with this, we have analyzed data from an age-structured model (the RAS [Realistic Age-Structured] model) with discrete school terms and found that the realized transmission rates also here decline through the term as a consequence of the heterogeneity induced by age structure (B. Finkenstadt and B. Grenfell, *unpublished results*). Earn et al. (2000) develop this further to show that age structure can theoretically be collapsed to a simple homogenous-mixing model by making the transmission parameters variable with time. This set of results offers a way to understand the systematic temporal variation in transmission rates. At a deeper level, Earn et al.'s (2000) result motivates how we can fit a nonstructured model, such as that described by Eqs. 1–4, to a phenomenon that is known to be age structured; the nonstructured model with transformed transmission coefficients may be thought of as having an implicit age structure.

Discrete time modeling

In response to Fine and Clarkson's (1982*a*) original discrete time model, Mollison and Din (1993) argued that the characteristic time scale of measles might be somewhat less than 14 d. To explore whether our results depend critically on the characteristic time scale, we carried out an analysis using 36 time steps/yr (just over 10-d time steps). Since the data are reported on a weekly basis, we obtained 10-d step time series by fitting an interpolating (cubic) spline through each time series and then integrating within each 10-d time step. (This inevitably introduces an additional level of sampling error because the output interval [10 d] is not a multiple of the observational interval [7 d]. The results appear to be qualitatively robust to this added error). Applying susceptible reconstruction and the TSIR model to this new set of data, we find that most parameter estimates are unaffected. The mixing coefficient, α, is still close to unity (mean = 0.96, SE = 0.01); The seasonal pattern of transmission maps closely onto that revealed by the 14-d analysis; The mean transmission is, on average, 20% lower (the expectation given the shorter epidemic period is 29%), and scales inversely with population size. We have also checked that the dynamic behavior of the 10-d model corresponds to that of the 14-d model—annual cycles for high birth rates and/or low seasonality and biannual cycles for low birth rates and/or high seasonality (Grenfell et al. 2002).

The two parameters that do appear to depend on time step length are the reproductive ratio, R_0, and the mean number of susceptibles, $\bar{S}$. The profile likelihood estimates of the mean proportion of susceptibles based on the 10-d model range from 3.5% to 8.5% with a global mean of 5.0% (SE = 0.1%). The estimates are more heterogeneous than for the 14-d analysis. This is possibly due to the error added through the re-aggregation of the data. The estimated proportions for the four larger cities (London, Birmingham, Liverpool, and Manchester) are 7.1%, 5.9%, 7.2%, and 6.0%, respectively. These estimates are closer to, but still significantly lower than, the 9% level concluded by Fine and Clarkson (1982*b*).

The invariance of R_0 with population size remains for 10-d-based estimates. The estimates, however, have lower precision for all but the biggest cities. In the four biggest cities the mean R_0 is estimated to 17.9, 18.8,

17.6, and 16.8—estimates in close agreement with the conventionally accepted values for prevaccination measles. Thus, future analysis of the TSIR model in conjunction with age-structured serological data, and more detailed clinical data may be needed. Fortunately, all but two of the parameters are robust to the characteristic time scale of the infection.

We have used a discrete time model to understand a process that is inherently continuous in time. Preliminary work comparing the TSIR model and a continuous-time SIR model with mass action transmission (K. Glass and B. Grenfell, *unpublished manuscript*), indicates that reducing α slightly below unity in the former may act as a correction for the discretization of the continuous-time infectious process. However, with careful choice of α (K. Glass and B. Grenfell, *unpublished manuscript*), the dynamics of the TSIR model is qualitative and quantitative mirroring the behavior (including bifurcation patterns and existence of multiple attractors) to the continuous-time age-structured model (Earn et al. 2000). A separate motivation for the discrete model is provided by the strong pulsing of the dynamics associated with school transmission (especially weekend breaks), and the relatively low variances in the durations of the incubation and infectious periods (Keeling 1997). The detailed high-frequency signature in the data (Keeling and Grenfell 1997) testifies to some level of generation separation in the continuous-time process. (For further discussion of generation separation in continuous systems see Gurney and Nisbet 1985, Jansen et al. 1990). However, to acknowledge the continuous nature of the birth–death process, we have formulated the model with a conditional variance (the negative binomial) as predicted from the theory of a discretely sampled continuous-time birth–death process (Kendall 1949). The model may therefore also be seen as a generalized birth–death process that is approximated by a piecewise (simple) constant birth–death process. Further formal comparisons of these models are in progress.

In conclusion, this paper illustrates the simple epidemic clockwork that underlies the dramatic cyclical behavior of measles. The patterns themselves, and their implications for vaccination, have generated a large and distinguished literature, in both modeling and data analysis. Here, we have developed a mechanistic time-series model that makes a first step towards unifying these approaches. The model captures the short-term (generation step) behavior of our 60 city data set remarkably well. In particular, it allows us to explore, in the largest such analysis to date, the scaling of epidemiological parameters with population size across three orders of magnitude in host population size. In a companion paper (Grenfell et al. 2002) we show how the TSIR model captures the long-term dynamical behavior of measles, and discuss how the balance between noise and determinism scales in this highly nonlinear ecological system.

Acknowledgments

O. N. Bjørnstad was supported by the National Center for Ecological Analysis and Synthesis (a center funded by NSF Grant #DEB-94-21535, the University of California Santa Barbara, and the State of California) and the Norwegian Science Foundation. B. T. Grenfell and B. F. Finkenstädt were supported financially by the Wellcome Trust. We thank Ben Bolker, Roger Nisbet, and one anonymous reviewer for valuable comments on the manuscript.

Literature Cited

Anderson, R. M. 1978. The regulation of host population growth by parasitic species. Parasitology **76**:119–157.

Anderson, R. M. 1982. Directly transmitted viral and bacterial infections of man. Pages 1–37 *in* R. M. Anderson, editor. Population dynamics of infectious diseases: theory and applications. Chapman and Hall, London, UK.

Anderson, R. M., H. C. Jackson, R. M. May, and A. M. Smith. 1981. Population dynamics of fox rabies in Europe. Nature **289**:765–771.

Anderson, R. M., and R. M. May. 1979. Population biology of infectious diseases: Part I. Nature **280**:361–367.

Anderson, R. M., and R. M. May. 1991. Infectious diseases of humans: dynamics and control. Oxford University Press, Oxford, UK.

Bailey, N. T. J. 1957. The mathematical theory of epidemics. Griffin, London, UK.

Barrett, T. 1987. The molecular biology of the morbillivirus (measles) group. Biochemical Society Symposium **53**:25–37.

Bartlett, M. S. 1956. Deterministic and stochastic models for recurrent epidemics. Pages 81–109 *in* J. Neyman, editor. Proceedings of the Third Berkely Symposium on Mathematical Statistics and Probability. University of California Press, Berkeley, California, USA.

Bartlett, M. S. 1957. Measles periodicity and community size. Journal of Royal Statistical Society A **120**:48–70.

Bartlett, M. S. 1960*a*. The critical community size for measles in the U.S. Journal of Royal Statistical Society A **123**: 37–44.

Bartlett, M. S. 1960*b*. Stochastic population models in ecology and epidemiology. Metheuen and Company Ltd., London, UK.

Begon, M., S. M. Feore, K. Brown, J. Chantrey, T. Jones, and M. Bennett. 1998. Population and transmission dynamics of cowpox in bank voles: testing fundamental assumptions. Ecology Letters **1**:82–86.

Begon, M., S. M. Hazel, D. Baxby, K. Bown, R. Cavanagh, J. Chantrey, T. Jones, and M. Bennett. 1999. Transmission dynamics of a zoonotic pathogen within and between wildlife host species. Proceedings of the Royal Society of London B **266**:1939–1945.

Bjørnstad, O. N., J.-M. Fromentin, N. C. Stenseth, and J. Gjøsæter. 1999. Cycles and trends in cod population. Proceedings of the National Academy of Science USA **96**: 5066–5071.

Black, F. L. 1984. Measles. Pages 397–418 *in* A. S. Evans, editor. Viral infections of humans: epidemiology and control. Plenum, New York, New York, USA.

Bobashev, G. V., S. P. Ellner, D. Nychka, and B. T. Grenfell. 2000. Reconstructing susceptible and recruitment dynamics from measles epidemic data. Mathematical Population Studies **8**:1–29.

Bolker, B. M., and B. T. Grenfell. 1993. Chaos and biological complexity in measles dynamics. Proceedings of the Royal Society of London B **251**:75–81.

Bolker, B. M., and B. T. Grenfell. 1996. Impact of vaccination on the spatial correlation and persistence of measles dynamics. Proceedings of the National Academy of Science USA **93**:12648–12653.

Casdagli, M. 1991. Chaos and deterministic versus stochastic non-linear modelling. Journal of Royal Statistical Society B **54**:303–328.

Clarkson, J. A., and P. E. M. Fine. 1985. The efficiency of measles and pertussis notification in England and Wales. International Journal of Epidemiology **14**:153–168.

Cliff, A. D., P. Haggett, and M. Smallman-Raynor. 1993. Measles: an historical geography of a major human viral disease from global expansion to local retreat, 1840–1990. Blackwell, Oxford, UK.

de Jong, M., O. Diekmann, and H. Heesterbeek. 1995. How does transmission of infection depend on population size? Pages 84–94 *in* D. Mollison, editor. Epidemic models: their structure and relation to data. Cambridge University Press, Cambridge, UK.

Diekmann, O., M. C. M. de Jong, A. A. de Koeijer, and P. Reijnders. 1996. The force of infection in populations of varying size: a modelling problem. Journal of Biological Systems **3**:519–529.

Dietz, K. 1976. The incidence of infectious diseases under the influence of seasonal fluctuations. Lecture Notes in Biomathematics **11**:1–15.

Dietz, K., and D. Schenzle. 1985. Mathematical models for infectious disease statistics. Pages 167–204 *in* A. C. Atkinson and S. E. Feinberg, editors. A celebration of statistics. Springer-Verlag, New York, New York, USA.

Drepper, F. R., R. Engbert, and N. Stollenwerk. 1994. Nonlinear time-series analysis of empirical population-dynamics. Ecological Modelling **75/76**:171–181.

Earn, D. J. D., P. Rohani, B. M. Bolker, and B. T. Grenfell. 2000. A simple model for complex dynamical transitions in epidemics. Science **287**:667–670.

Earn, D. J. D., P. Rohani, and B. T. Grenfell. 1998. Persistence, chaos and synchrony in ecology and epidemiology. Proceedings of the Royal Society of London B **265**:7–10.

Ellner, S. P., B. A. Bailey, G. V. Bobashev, A. R. Gallant, B. T. Grenfell, and D. W. Nychka. 1998. Noise and nonlinearity in measles epidemics: combining mechanistic and statistical approaches to population modeling. American Naturalist **151**:425–440.

Ellner, S., A. R. Gallant, and J. Theiler. 1995. Detecting nonlinearity and chaos in epidemic data *in* D. Mollison, editor. Epidemic models: their structure and relation to data. Cambridge University Press, Cambridge, UK.

Evans, M., N. Hastings, and B. Peacock. 1993. Statistical distributions. Second edition. John Wiley, New York, New York, USA.

Fine, P. E. M., and J. A. Clarkson. 1982*a*. Measles in England and Wales. I. An analysis of factors underlying seasonal patterns. International Journal of Epidemiology **11**:5–15.

Fine, P. E. M., and J. A. Clarkson. 1982*b*. Measles in England and Wales. II. The impact on measles vaccination programme on the distribution of immunity in the population. International Journal of Epidemiology **11**:15–25.

Finkenstädt, B., O. N. Bjørnstad, and B. T. Grenfell. 2002. A stochastic model for extinction and recurrence of epidemics: estimation and inference for measles outbreaks. Biostatistics, *in press*.

Finkenstädt, B., and B. Grenfell. 1998. Empirical determinants of measles metapopulation dynamics in England and Wales. Proceedings of the Royal Society of London B **265**: 211–220.

Finkenstädt, B., and B. Grenfell. 2000. Time series modelling of childhood diseases: a dynamical systems approach. Applied Statistics **49**:187–205.

Finkenstädt, B., M. Keeling, and B. Grenfell. 1998. Patterns of density dependence in measles population dynamics. Proceedings of the Royal Society of London B **265**:753–762.

Grenfell, B. T. 1992. Chance and chaos in measles dynamics. Journal of Royal Statistical Society B **54**:383–398.

Grenfell, B. T., and R. M. Anderson. 1985. The estimation of age-related rates of infection from case notifications and serological data. Journal of Hygiene (Cambridge) **95**:419–436.

Grenfell, B. T., O. N. Bjørnstad, and B. Finkenstädt. 2002. Dynamics of measles epidemics: scaling noise, determinism, and predictability with the TSIR model. Ecological Monographs **72**:185–202.

Grenfell, B. T., O. N. Bjørnstad, and J. Kappey. 2001. Travelling waves and spatial hierarchies in measles epidemics. Nature **414**:716–723.

Grenfell, B. T., and B. M. Bolker. 1998. Cities and villages: infection hierarchies in a measles metapopulation. Ecology Letters **1**:63–70.

Grenfell, B. T., and A. P. Dobson. 1995. Ecology of infectious diseases in natural populations. Cambridge University Press, Cambridge, UK.

Grenfell, B. T., and J. Harwood. 1997. (Meta)population dynamics of infectious diseases. Trends in Ecology and Evolution **12**:395–399.

Grenfell, B. T., A. Kleczkowski, and B. M. Bolker. 1995. Seasonality, demography and the dynamics of measles in developed countries. Pages 248–268 *in* D. Mollison, editor. Epidemic models: their structure and relation to data. Cambridge University Press, Cambridge, UK.

Grenfell, B. T., A. Kleczkowski, S. P. Ellner, and B. M. Bolker. 1994. Measles as a case study in nonlinear forecasting and chaos. Philosophical Transactions of the Royal Society London A **348**:515–530.

Gurney, W. S. C., and R. M. Nisbet. 1985. Fluctuation periodicity, generation separation, and the expression of larval competition. Theoretical Population Biology **28**:150–180.

Hanski, I. 1998. Metapopulation dynamics. Nature **396**:41–49.

Heesterbeek, J. A. P., and M. G. Roberts. 1994. Mathematical models for microparasites of wildlife. Pages 90–122 *in* B. T. Grenfell and A. P. Dobson, editors. Infectious diseases in natural populations. Cambridge University Press, Cambridge, UK.

Hilborn, R., and M. Mangel. 1997. The ecological detective. Princeton University Press, Princeton, New Jersey, USA.

Jansen, V. A. A., R. M. Nisbet, and W. S. C. Gurney. 1990. Generation cycles in stage structured populations. Bulletin of Mathematical Biology **52**:375–396.

Keeling, M. J. 1997. Modelling the persistence of measles. Trends in Microbiology **5**:513–518.

Keeling, M. J., and B. T. Grenfell. 1997. Disease extinction and community size: modeling the persistence of measles. Science **275**:65–67.

Kendall, B. E., W. M. Schaffer, L. F. Olsen, C. W. Tidd, and B. L. Jorgensen. 1994. Using chaos to understand biological dynamics. Pages 184–203 *in* J. Grasman and G. van Straten, editors. Predictability and nonlinear modelling in natural sciences and economics. Kluwer Academic Publishers, Dordrecht, The Netherlands.

Kendall, D. G. 1949. Stochastic processes and population growth. Journal of Royal Statistical Society B **11**:230–264.

Keyfitz, N., and G. Littman. 1980. Mortality in a heterogenous population. Population Studies **33**:333–342.

Liu, W. M., H. W. Hethcote, and S. A. Levin. 1987. Dynamical behaviour of epidemiological models with nonlinear incidence rates. Journal of Mathematical Biology **25**:359–380.

Liu, W. M., Y. Iwasa, and S. A. Levin. 1986. Influence of nonlinear incidence rates upon the behaviour of SIRS epidemiological models. Journal of Mathematical Biology **23**: 187–204.

May, R. M., and R. M. Anderson. 1978. Regulation and stability of host–parasite population interactions. II. Destabilizing processes. Journal of Animal Ecology **47**:249–267.

May, R. M., and R. M. Anderson. 1979. Population biology of infectious diseases: Part II. Nature **280**:455–461.

McCallum, H., N. Barlow, and J. Hone. 2001. How should pathogen transmission be modelled? Trends in Ecology and Evolution **16**:295–300.

McLean, A. R., and R. M. Anderson. 1988. Measles in developing countries. Part I. Epidemiological parameters and patterns. Epidemiology and Infection **100**:11–133.

Mollison, D., and S. U. Din. 1993. Deterministic and stochastic models for the seasonal variability of measles transmission. Mathematical Biosciences **117**:155–177.

Murphy, S. A., and A. W. Van der Vaart. 2000. On profile likelihood. Journal of the American Statistical Association **95**:449–465.

Murray, G. D., and A. D. Cliff. 1975. A stochastic model for measles epidemics in a multi-region setting. Institute of British Geographers **2**:158–174.

Olsen, L. F., and W. M. Schaffer. 1990. Chaos versus noisy periodicity: alternative hypotheses for childhood epidemics. Science **249**:499–504.

Olsen, L. F., G. L. Truty, and W. M. Schaffer. 1988. Oscillations and chaos in epidemics: a nonlinear dynamic study of six childhood diseases in Copenhagen, Denmark. Theoretical Population Biology **33**:344–370.

Rand, D. A., and H. B. Wilson. 1991. Chaotic stochasticity: a ubiquitous source of unpredictability in epidemics. Proceedings of the Royal Society of London B **246**:179–184.

Renshaw, E. 1991. Modelling biological populations in space and time. Cambridge University Press, Cambridge, UK.

Rhodes, C. J., and R. M. Anderson. 1996*a*. Power laws governing epidemics in isolated populations. Nature **381**:600–602.

Rhodes, C. J., and R. M. Anderson. 1996*b*. A scaling analysis of measles epidemics in a small population. Philosophical Transactions of the Royal Society London B **351**:1679–1688.

Rohani, P., D. J. Earn, B. Finkenstadt, and B. T. Grenfell. 1998. Population dynamic interference among childhood diseases. Proceedings of the Royal Society of London B **265**:2033–2041.

Schaffer, W. M., and M. Kot. 1985. Nearly one dimensional dynamics in an epidemic. Journal of Theoretical Biology **112**:403–427.

Schenzle, D. 1984. An age-structured model of pre- and post-vaccination measles transmission. IMA Journal of Mathematics Applied in Medicine and Biology **1**:169–191.

Schwartz, I. B. 1985. Multiple recurrent outbreaks and predictability in seasonally forced nonlinear epidemic models. Journal of Mathematical Biology **21**:347–361.

Shea, K., P. H. Thrall, and J. J. Burdon. 2000. An integrated approach to management in epidemiology and pest control. Ecology Letters **3**:150–158.

Silverman, B. W. 1986. Density estimation for statistics and data analysis. Chapman and Hall, London, UK.

Stone, L. 1992. Coloured noise or low-dimensional chaos. Proceedings of the Royal Society of London B **250**:77–81.

Stone, L., G. Landan, and R. M. May. 1996. Detecting time's arrow: a method for identifying nonlinearity and deterministic chaos in time-series data. Proceedings of the Royal Society of London B **263**:1509–1513.

Sugihara, G., B. Grenfell, and R. M. May. 1990. Distinguishing error from chaos in ecological time series. Philosophical Transactions of the Royal Society London B **330**: 235–251.

Sugihara, G., and R. M. May. 1990. Nonlinear forecasting as a way of distinguishing chaos from measurement error in time series. Nature **344**:734–741.

Swinton, J., C. A. Gilligan, J. Harwood, and A. Hall. 2002. Scaling of phocine distemper virus transmission with harbour seal community size. Ecologie, *in press.*

Vaupel, J. W., K. G. Manton, and E. Stallard. 1979. The impact of heterogeneity in individual frailty on the dynamics of mortality. Demography **16**:439–454.

Vaupel, J. W., and A. N. Yashin. 1985. Heterogeneity's ruses: some surprising effects of selection on population dynamics. American Statistician **39**:176–185.

APPENDIX A

A description of the assumptions made in order to estimate the parameters of disease transmission in Eq. 1 is available in ESA's Electronic Data Archive: *Ecological Archives* M072-002-A1.

APPENDIX B

The development of the estimating equation is available in ESA's Electronic Data Archive: *Ecological Archives* M072-002-A2.